Journal of Biomolecular NMR, **26:** 13–24, 2003.
KLUWER/ESCOM

Broadband RFDR with adiabatic inversion pulses

Jörg Leppert, Bert Heise, Oliver Ohlenschläger, Matthias Görlach & Ramadurai Ramachandran*
Abteilung Molekulare Biophysik/NMR-Spektroskopie, Institut für Molekulare Biotechnologie, 07745 Jena, Germany

Received 2 October 2002; Accepted 28 January 2003

Key words: adiabatic pulse, chemical shift correlation, RFDR, solid state NMR

Abstract

With a view to obtain ^{13}C chemical shift correlation spectra of uniformly labelled peptides/proteins at high magnetic fields and high magic angle spinning frequencies ($\omega_r/2\pi \leq 20$ kHz), the efficacy of RFDR with adiabatic inversion pulses has been assessed via numerical simulations and experimental measurements employing different adiabatic pulse phasing schemes, shapes and durations. It is demonstrated that homonuclear dipolar recoupling with superior performance under resonance offset and H_1 inhomogeneity effects and without strong dependence on the ^{13}C chemical shift differences can be achieved with adiabatic pulses. It is shown that ^{13}C chemical shift correlation spectra in the entire range of carbon chemical shifts can be obtained efficiently with short adiabatic inversion pulses. In situations where correlation spectra of only the aliphatic region are required, the possibility for minimising the interference between the recoupling and decoupling RF fields with long adiabatic pulses, at low recoupling power levels and without compromising the broadband RFDR characteristics, is also indicated.

Introduction

Radio Frequency Driven Recoupling (RFDR) (Bennett et al., 1992, 1998) with longitudinal magnetisation exchange is increasingly being used for generating homonuclear ^{13}C chemical shift correlation spectra in biological systems at high fields (Boender et al., 1995; McDermott et al., 2000; Pauli et al., 2000; Pauli et al., 2001; van Rossum et al., 2002). With short dipolar recoupling times, spins in spatial proximity (e.g., one-bond distance) lead to cross peaks in such spectral data. Hence, in a peptide/protein, various amino acid residues with differing clusters of nearby ^{13}C nuclei show characteristic chemical shift connectivity patterns. This facilitates the assignment of ^{13}C resonances to specific amino acid types. Dipolar recoupling in RFDR is typically achieved via the application of rotor-synchronised rectangular 180° pulses, with the phases of the inversion pulses being suitably cycled to achieve efficient recovery of single spin magnetisations and to generate an effective dipolar Hamiltonian. In RFDR, the ^{1}H decoupling field generally employed, both at short as well as long mixing times, is three times as strong as the ^{13}C RF field so as to avoid signal losses due to the interference between the decoupling and recoupling RF fields (Bennett et al., 1998; Zaborowski et al., 1999). At magnetic field strengths corresponding to a ^{1}H frequency in the range of 750–900 MHz the ^{13}C chemical shift correlation spectrum of a protein would span a frequency range of 30–40 kHz. In situations where the available ^{1}H decoupling power is limited it could become difficult to generate efficiently chemical shift correlation spectra in the entire range of ^{13}C chemical shifts with RFDR employing conventional rectangular 180° pulses. With a view to eliminate resonance offset and H_1 inhomogeneity effects, we have been exploring the potential of adiabatic inversion pulses (Baum et al., 1985; Kupce and Freeman, 1995, 1996; Tannus and Garwood, 1996; Hwang et al., 1998) in dipolar recoupling experiments (Heise et al., 2000, 2002; Leppert, 2001; Heise, 2001; Leppert et al., 2002).

*To whom correspondence should be addressed. E-mail: raman@imb-jena.de

RFDR experiments with rectangular inversion pulses are typically carried out with the xy phasing scheme (Gullion et al., 1990). Our recent experimental studies have shown that the p5 phasing scheme {0°, 150°, 60°, 150°, 0°}, originally designed to achieve broadband inversion of longitudinal magnetisations (Tycko et al., 1985; Fujiwara and Nagayama, 1988), can also be effectively employed for dipolar recoupling with adiabatic inversion pulses (Heise et al., 2002). A variety of other phase cycles such as the p5a {0°, 330°, 60°, 330°, 0°}, p5b {0°, 0°, 120°, 60°, 120°}, p5c {0°, 120°, 0°, 60°, 240°}, p5d {0°, 240°, 240°, 60°, 0°}, p7 {0°, 105°, 300°, 255°, 300°, 105°, 0°} and p9 {0°, 15°, 180°, 165°, 270°, 165°, 180°, 15°, 0°} (Tycko et al., 1985) are available for broadband adiabatic inversion of longitudinal magnetisations and hence it is of interest to assess the relative merits of different phasing schemes for RFDR with adiabatic pulses.

With many biological systems it may be difficult to employ very fast spinning speeds, for example to avoid sample dehydration (McDermott et al., 2000), and hence it may be necessary to record RFDR data only at spinning frequencies in the range of $\omega_r/2\pi \sim$ 10–20 kHz or less. Even at these spinning speeds, it is conceivable that adiabatic inversion pulses would occupy a significant fraction of the rotor period and thereby could affect, for better or worse, the RFDR performance characteristics. To minimise the interference between decoupling and recoupling RF fields, it would be advantageous to employ adiabatic inversion pulses of long duration as they generally require less RF power for satisfying the adiabatic threshold requirements. The application of rectangular inversion pulses of long duration would also require less RF power and hence reduce the interference between decoupling and recoupling fields. However, this would lead to a smaller excitation bandwidth and therefore to a reduction in the spectral range over which 2D chemical shift correlation data can be recorded. On the other hand, the inversion bandwidth does not necessarily get compromised with long adiabatic pulses. In this context, a knowledge of the dependence of the efficacy of RFDR on χ, the ratio of the adiabatic pulse width to the rotor period, becomes highly relevant. This will help in determining 'at any given spinning' speed the optimal adiabatic pulse width that can be employed without degrading significantly the efficacy of dipolar recoupling.

A variety of amplitude and frequency modulation functions with varying RF power/duty factors have been proposed for adiabatic inversion of longitudinal magnetisations (Kupce and Freeman, 1995, 1996; Hwang et al., 1998). Hence, it is of interest to have an understanding of the effects of adiabatic pulse shape on the recoupling dynamics. In view of the increasing usage of RFDR in the study of biological systems at high magnetic fields we have evaluated via numerical simulations and experimental measurements the performance characteristics of RFDR with adiabatic inversion pulses.

Experimental and numerical procedures

The RFDR sequence employed in this work is shown in Figure 1. All experiments were performed with an undiluted, uniformly ^{13}C and ^{15}N labelled sample of alanine at room temperature on a 500 MHz wide bore Varian $^{\text{UNITY}}$*INOVA* solid state NMR spectrometer equipped with a 5-mm DOTY supersonic triple resonance probe and waveform generators for pulse shaping. Cross-polarization under Hartmann-Hahn matching conditions was employed and all spectra, unless mentioned otherwise, were collected under high power ^1H decoupling (~90 kHz). Typical ^1H and ^{13}C 90° pulse widths were 2.8 and 5.3 μs, respectively. In this study we have employed the tanh/tan adiabatic inversion pulse (Hwang et al., 1998) constructed from the following adiabatic half passage and its time reversed half passage:

$$\omega_1(t) = \omega_1(\text{max}) \tanh[\xi 2t/T_p]$$

$$\Delta\omega(t) = \Delta\omega_{\text{max}}[\tan(\kappa(1 - 2t/T_p))]/\tan(\kappa),$$

where $\xi = 10$, $\tan(\kappa) = 20$ and $0 \leq t \leq T_p/2$. Additionally, to assess the dependence of the dipolar recoupling efficiency on the nature of the adiabatic pulse profile, we have also employed the constant adiabaticity inversion pulse 'cagauss' as implemented in the Varian pulse shaping software 'Pbox'. The cagauss pulse is defined by the modulation profiles:

$$\omega_1(t) = \omega_1(\text{max}) \exp(-\beta t^2)$$

$$\Delta\omega(t) = \lambda \text{erf}(\beta t),$$

where λ and β are defined as

$$\lambda = [\omega_1(\text{max})]^2/\beta Q$$

and

$$\beta = (1/\tau\sqrt{-\ln(a_{\text{tr}})},$$

where Q is the adiabaticity parameter (Kupce and Freeman, 1996), 2τ is the total duration of the pulse

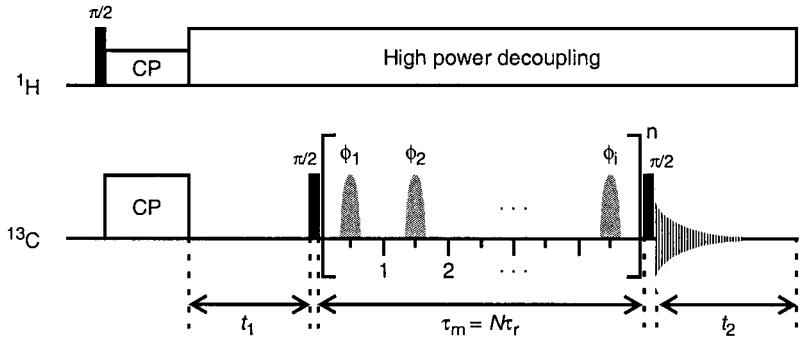

Figure 1. RFDR pulse sequence employed in this work. Homonuclear dipolar recoupling is achieved by applying an inversion pulse at the center of each rotor period, with the phases of the inversion pulses cycled suitably (see text).

and a_{tr} is the truncation parameter ($0 < a_{tr} < 1.0$). A Q value of 4 and $a_{tr} = 0.01$ were employed in this work. All tanh/tan adiabatic pulses employed in this work had an R value, representing the product of the pulse bandwidth and the pulse length (Hwang et al., 1998) of 60. The cagauss pulses uniformly had a duration of 80 μs (ω_1(max) = 42 kHz) and a frequency sweep width of 80 kHz. The frequency sweep is implemented in the spectrometer hardware as a phase modulation, $\delta(t) = \int \Delta\omega(t)dt$. Adiabatic pulses were typically divided into 200 slices of equal duration with each slice characterised by an amplitude and phase parameter. Numerical simulations were carried out using the SIMPSON program (Bak et al., 2000) and considering two representative spin 1/2 systems in a uniformly labelled peptide/protein. The first case corresponds to homonuclear dipolar recoupling between the $^{13}C'$ and $^{13}C^{\alpha}$ sites and the other corresponds to the $^{13}C^{\alpha}$ and $^{13}C^{\beta}$ sites. Unless mentioned otherwise, ^{13}C chemical shift (CS) tensor and dipolar coupling parameters of glycine and alanine essentially as used by Brinkmann et al. (2002) were employed, respectively, in these calculations. Although results obtained from simulations carried out for the two spin systems may not possibly hold good exactly for multi-spin systems, general conclusions about the merits of RFDR with adiabatic pulses can still be reached. Our approach is similar to the general practice followed in the literature (Brinkmann et al., 2002). All simulations were performed taking into account scalar coupling interactions and employing RF field strengths available in our 5-mm MAS NMR probes. Unless otherwise mentioned, the RF carrier was kept at the middle of the two sites in these simulations. Simulations have been carried out at two representative field strengths corresponding to ^{1}H frequencies of 500 and 800 MHz and employing representative spinning speeds of 11 000 and 15 000 Hz, respectively. The powder averaging was done by choosing 256 (α, β) values according to the REPULSION distribution scheme (Bak and Nielsen, 1997) and 16 γ values.

Results and discussion

The efficacy of RFDR with adiabatic pulses has been assessed by monitoring the magnitude of longitudinal magnetisation transferred to the second spin ($^{13}C'$/$^{13}C^{\beta}$) as a function of the dipolar mixing time, starting with z magnetisation on spin 1 ($^{13}C^{\alpha}$) at zero recoupling time. As an example, the simulated data obtained with rectangular inversion pulses of 13.4 μs duration ($\gamma H_1 = 37.3$ kHz) employing the xy-8 phasing scheme are also given for comparison.

Figure 2 shows the efficacy of RFDR with different adiabatic phasing schemes. These simulations were carried out employing tanh/tan adiabatic pulses of 40 μs duration with an RF field strength, ω_1 (max)/2π, of 37.3 kHz. Although simulations were carried out employing all p5 phasing schemes mentioned earlier, for the sake of clarity only a few representative plots are given. The initial rate of transfer of magnetisation from one spin to another is a measure of the efficacy of dipolar recoupling, with a faster transfer representing an efficient dipolar recoupling. From the simulations given in Figure 2, it is seen that the initial rate of transfer of magnetisation from the C^{α} to the C^{β} spin is faster with the adiabatic pulses compared to that with the rectangular pulses. The $C^{\alpha} \rightarrow C'$ initial buildup rates are similar for the two cases, although the RFDR performance with the rectangular pulses is not satisfactory at longer mixing times, possibly due to their poor inversion bandwidth. For short mixing times, in general, all adiabatic pulse phasing schemes

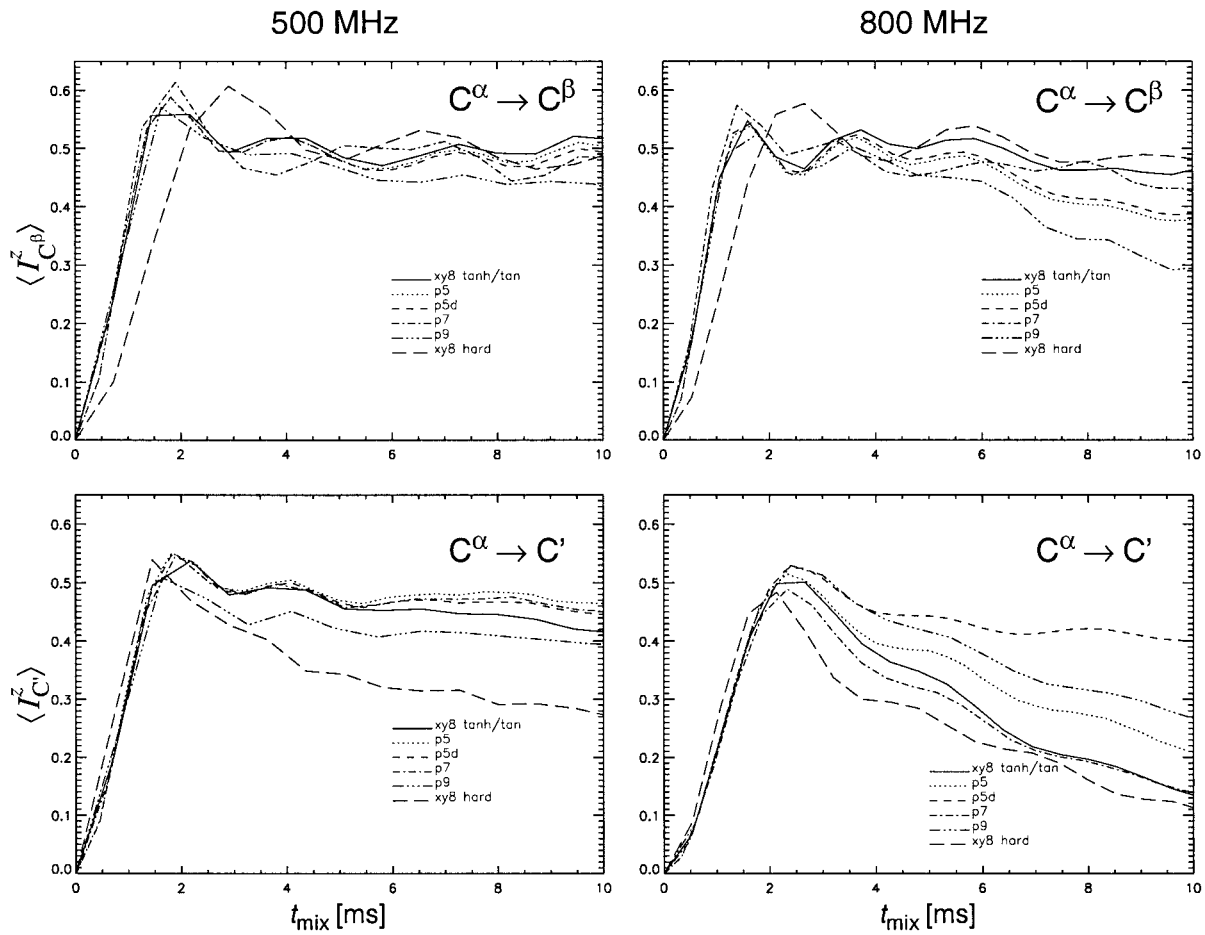

Figure 2. Simulated longitudinal magnetisation transfer characteristics of the RFDR sequence with different adiabatic pulse phasing schemes. These simulated plots show, at the field strengths indicated, the magnitude of the transferred magnetisation (normalised to the maximum transferable signal) on the second spin ($^{13}C'$/ $^{13}C^\beta$) starting with z magnetisation on spin 1 ($^{13}C^\alpha$) at zero recoupling time. Simulations at 500 and 800 MHz were carried out at spinning speeds of 11 000 and 15 000 Hz, respectively. For the $C^\alpha \rightarrow C^\beta$ and $C^\alpha \rightarrow C'$ transfers the following ^{13}C CS tensor, scalar and dipolar coupling parameters of alanine and glycine as employed by Brinkmann et al. (2002) were respectively used: Alanine (C^α: isotropic shift $\delta_{iso} = 50.9$ ppm, shift anisotropy $\delta_{aniso} = -19.67$ ppm, asymmetry parameter $\eta = 0.437$, Euler angles $\Omega_{PM} = \{81.7°, 24.5°, 29.1°\}$, C^β: $\delta_{iso} = 20.0$ ppm, $\delta_{aniso} = -11.7$ ppm, $\eta = 0.76$, $\Omega_{PM} = \{-52.9°, 77.4°, 140.5°\}$, dipolar coupling: $D = -2125$ Hz, $\Omega_{PM} = \{0°, 78.4°, 144.7°\}$, J-coupling: $J = 35$ Hz) and Glycine (C^α: $\delta_{iso} = 45.0$ ppm, $\delta_{aniso} = -19.43$ ppm, $\eta = 0.98$, $\Omega_{PM} = \{99.4°, 146.0°, 138.9°\}$, C': $\delta_{iso} = 178.2$ ppm, $\delta_{aniso} = -74.5$ ppm, $\eta = 0.88$, $\Omega_{PM} = \{-0.7°, 88.5°, 52.5°\}$, dipolar coupling: $D = -2135$ Hz, $\Omega_{PM} = \{0°, 0°, 0°\}$, J-coupling: $J = 53.1$ Hz). Euler angles have been defined with respect to a molecule-fixed frame M. In the case of glycine the molecule-fixed frame has its z-axis along the $^{13}C^\alpha$-$^{13}C'$ internuclear vector and in the case of alanine the molecule-fixed frame coincides with the crystallographic reference frame (Lehmann et al., 1972). The ^{13}C RF carrier was kept at the centre of the corresponding carbon resonances. Simulations were carried out in time increments of 5, 7, 8 or 9 rotor periods and the resulting data points, to provide visual clarity, have been simply joined. Simulations for the rectangular inversion pulse (13.4 µs, 37.3 kHz γH_1) were carried out with the xy-8 phasing scheme. The phasing schemes employed for the tanh/tan pulses (40 µs, 37.3 kHz γH_1) are indicated in the plots.

perform equally well. However, at longer mixing times substantial differences can be seen between the different phasing schemes, in particular for the $C^\alpha \rightarrow C'$ transfer. With increasing recoupling RF field strength, the performance characteristics of the different adiabatic pulse phasing schemes improve at longer mixing times (data not shown). To minimise the interference between the decoupling and recoupling RF fields, it will be advantageous to employ the phasing scheme that leads to optimal RFDR performance with minimal recoupling RF power. It can be inferred from Figure 2 that at high fields, in cases where it is desired to generate 2D ^{13}C chemical shift correlation data in the entire $\sim$ 180 ppm range including cross peaks arising from relayed magnetisation transfer, it will be advantageous to employ adiabatic pulses with the p5d instead of the

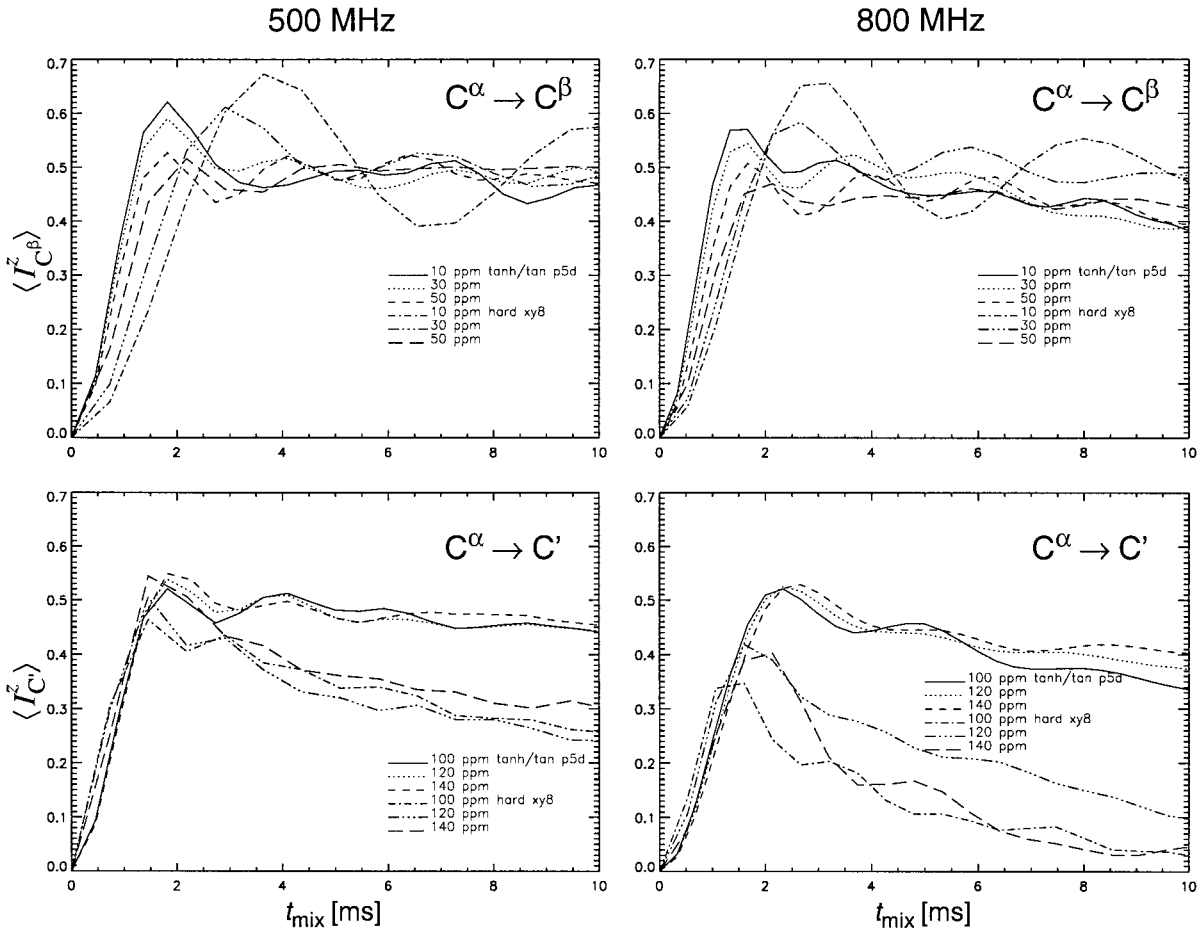

Figure 3. Simulated longitudinal magnetisation transfer characteristics of the RFDR sequence as a function of the indicated chemical shift difference between the recoupled nuclei. The plots for the tanh/tan pulses (40 μs, 37.3 kHz γH_1) were obtained with the p5d phasing scheme. All other parameters employed in the simulations are as in Figure 2.

xy-8 phasing scheme. P5d is seen to be even better than the p5 phasing scheme employed in our earlier studies (Heise et al., 2002). It is also worth mentioning here that the performance of the rectangular inversion pulses with the p5d phasing scheme and that of the adiabatic pulses with the xx phasing scheme are found to be very much inferior to the corresponding data given in Figure 2 (data not shown).

Figure 3 shows the RFDR performance as a function of the chemical shift difference between the recoupled nuclei. The plots with adiabatic pulses were generated with the p5d phasing scheme employing tanh/tan pulses (40 μs duration, $\omega_1(\mathrm{max})/2\pi$ = 37.3 kHz). With the adiabatic pulses, both at low and high fields/spinning speeds, it is seen that the initial buildup rates for the $C^\alpha \rightarrow C^\beta$ and $C^\alpha \rightarrow C'$ transfers are not strongly influenced by the chemical shift differences. This behaviour is similar to that observed with the finite pulse RFDR (fpRFDR) technique reported recently for RFDR at very fast magic angle spinning frequencies (∼ 20–40 kHz) (Ishii, 2001). When the chemical shift difference is smaller, the initial buildup rate is marginally faster for both $C^\alpha \rightarrow C^\beta$ and $C^\alpha \rightarrow C'$ transfers and for the $C^\alpha \rightarrow C^\beta$ transfer, the maximum amplitude of the exchanged magnetisation is marginally higher. Due to the differences in the magnitudes and orientations of the ^{13}C CS tensors of the two nuclei involved, the $C^\alpha \rightarrow C^\beta$ and $C^\alpha \rightarrow C'$ initial buildup rates are expected to be different and this can also be clearly seen in the 800 MHz RFDR simulations given in Figures 2 and 3. With adiabatic pulses, the $C^\alpha \rightarrow C^\beta$ transfer is faster than the $C^\alpha \rightarrow C'$ transfer. However, with a dipolar recoupling time of ∼ 2 ms (at the spinning speeds indicated) both

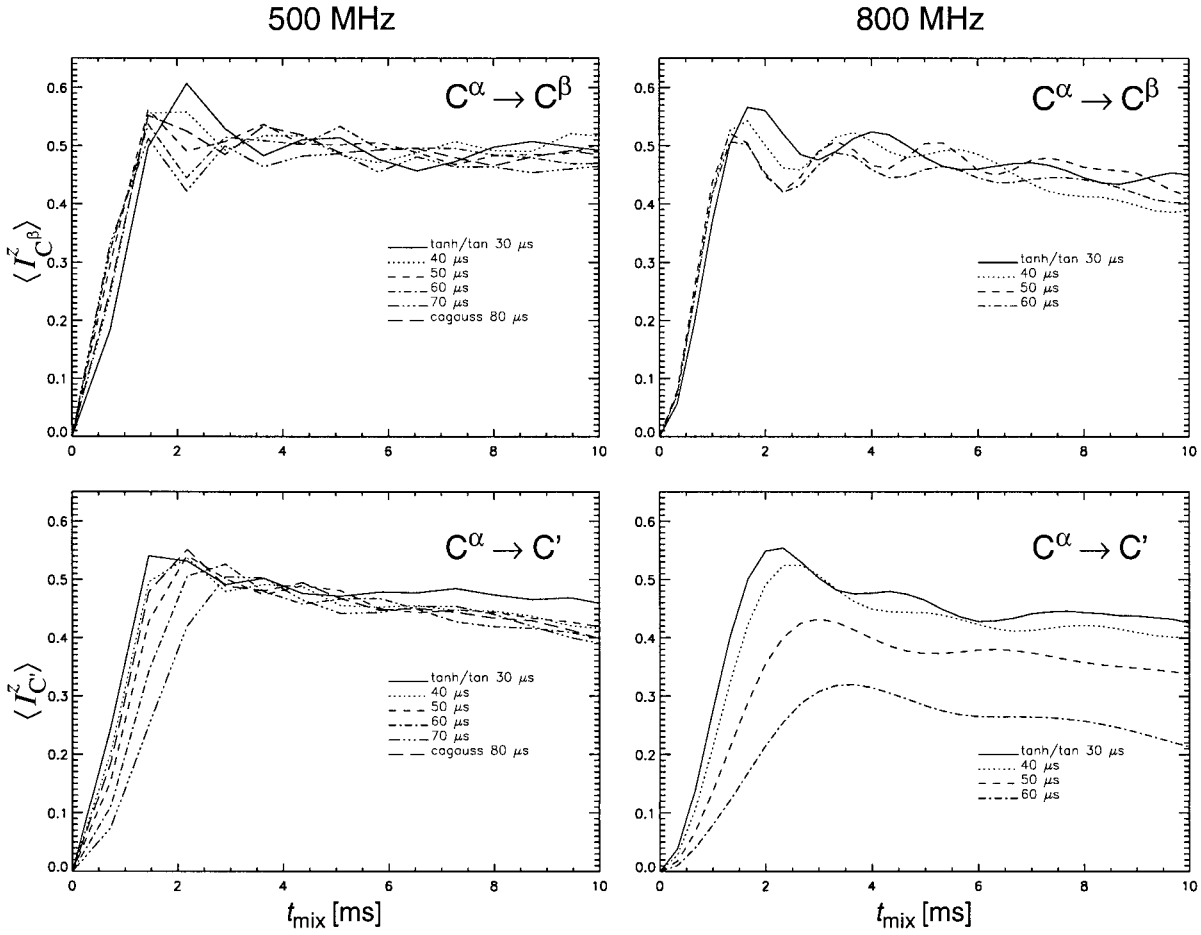

Figure 4. Simulated longitudinal magnetisation transfer characteristics of the RFDR sequence as a function of the tanh/tan adiabatic pulse widths indicated. Simulations were carried out with xy-8 and p5d phasing schemes at 500 MHz and 800 MHz, respectively. 80 μs cagauss pulses (ω_1(max)/2π = 42 kHz) and tanh/tan pulses with a duration of 30, 40, 50, 60 and 70 μs (ω_1(max)/2π = 47, 37.3, 33, 30 and 30 kHz, respectively) were employed. All other parameters employed in the simulations are as in Figure 2.

$C^\alpha \leftrightarrow C^\beta$ and $C^\alpha \leftrightarrow C'$ cross peaks of appreciable intensities should be seen in a 2D ^{13}C chemical shift correlation spectrum generated employing the adiabatic pulses. Although at short mixing times the RFDR performance with the rectangular pulses is seen to be satisfactory, at larger mixing times the performance with adiabatic pulses is highly superior. In the presence of significant resonance offset, as will be shown below, the performance of RFDR with the rectangular pulse is far from satisfactory even at short mixing times.

Figure 4 shows the effect of χ, the ratio of the width of the adiabatic pulses to the rotor period, on the RFDR performance. Simulations were carried out with xy-8 and p5d phasing schemes at 500 MHz and 800 MHz, respectively, and employing 80 μs cagauss pulses (ω_1(max)/2π = 42 kHz) and tanh/tan pulses with a duration of 30, 40, 50, 60 and 70 μs (ω_1(max)/2π = 47, 37, 33, 30 and 30 kHz, respectively). The RF pulse widths employed at the spinning speeds of 11 000 and 15 000 Hz represent a χ range of 0.33–0.88 and 0.45–0.9, respectively. The RF field strengths employed in these simulations correspond approximately to the values determined experimentally for the optimal performance of the RFDR sequence with the respective adiabatic pulses. For the $C^\alpha \rightarrow C^\beta$ transfer, it is seen that the effect of χ variations on the performance of RFDR is minimal and with an increase in χ the initial rate of buildup only increases, albeit marginally. That is, if one is interested in generating ^{13}C 2D chemical shift correlation data in the aliphatic region only, then it will

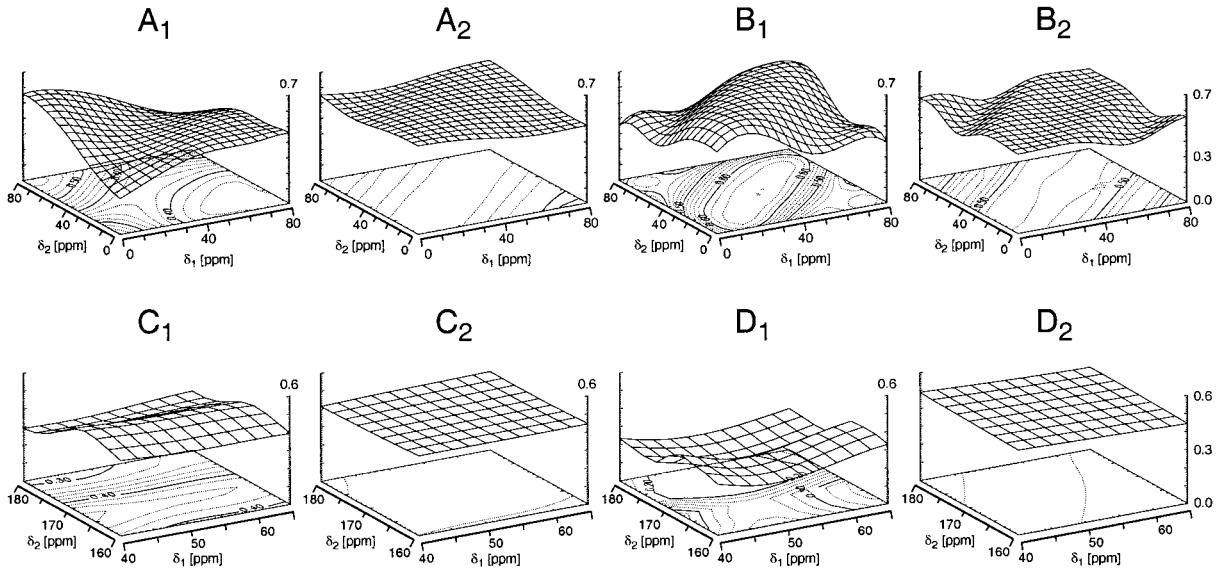

Figure 5. Transferred signal amplitude on the second spin $^{13}C^{\beta}$ (A1, A2, B1, B2) and $^{13}C'$ (C1, C2, D1, D2) starting with z magnetisation on spin 1 ($^{13}C^{\alpha}$) at zero recoupling time as a function of the isotropic chemical shifts δ_1 and δ_2 of the two nuclei. The plots for the 13.4 μs rectangular (A1, B1, C1, D1) and 40 μs tanh/tan inversion pulses (A2, B2, C2, D2) were obtained employing xy-8 and p5d phasing schemes, respectively, at 800 MHz and at a spinning speed of 15 000 Hz. Dipolar recoupling times of 1.6 ms (A1, C1) and 3.2 ms (B1, D1) were employed with the rectangular inversion pulse. Mixing times of 1.67 ms (A2, C2) and 3.33 ms (B2, D2) were employed with the adiabatic pulse. All other parameters are as in Figure 2. For the $C^{\alpha} \rightarrow C^{\beta}$ and $C^{\alpha} \rightarrow C'$ transfers the ^{13}C RF carrier frequencies were kept at 40 and 100 ppm, respectively.

be advantageous to employ adiabatic pulses of longer duration as they require only a lower RF field strength for obtaining satisfactory RFDR performance. On the other hand, with the tanh/tan pulses the $C^{\alpha} \rightarrow C'$ transfer rate significantly deteriorates with increasing χ. However, the initial $C^{\alpha} \rightarrow C'$ transfer rate observed with 80 μs cagauss pulses, having a smaller RF power/duty factor in comparison to the tanh/tan pulse of similar duration, is as good as that obtained with 40 μs tanh/tan pulses. Hence, it appears that it will be advantageous to employ in RFDR experiments, spinning speeds permitting, adiabatic pulses with smaller RF power/duty factor such as 'cagauss'. A potential advantage with such pulses is that, although the peak RF field strength requirements are larger, the interference between the recoupling and decoupling fields, due to the smaller RF power/duty factor, will be less in comparison to tanh/tan pulses of similar duration. Although the RFDR simulations with adiabatic pulses shown in Figures 2–4 were carried out employing the basic phase cycles, simulations have also been carried out employing supercycles such as p5$\overline{\text{p5}}$. However, no significant differences were seen in the longitudinal magnetisation transfer characteristics (data not shown).

Figure 5 shows a few representative plots of the magnitude of the transferred longitudinal magnetisation on spin 2 as a function of the isotropic chemical shifts δ_1 and δ_2 of the dipolar coupled nuclei. These plots, corresponding to a spinning speed of 15 000 Hz, a field strength of 800 MHz and two different mixing times were obtained employing rectangular and tanh/tan inversion pulses of 13.4 μs and 40 μs duration with xy-8 and p5d phasing schemes, respectively. For $C^{\alpha} \rightarrow C^{\beta}$ and $C^{\alpha} \rightarrow C'$ transfers the carrier frequencies were kept at 40 and 100 ppm, respectively. From these plots it is seen that the performance of RFDR with adiabatic pulses is superior and that the longitudinal magnetisation transfer characteristics with adiabatic pulses is not very much dependent on chemical shift differences of the dipolar coupled nuclei. The plots shown for the $C^{\alpha} \rightarrow C^{\beta}$ transfer correspond approximately to a situation where the ^{13}C carrier is kept at the middle of the aliphatic carbon chemical shift range. However, if one is interested in generating 2D chemical shift correlation data in the entire ^{13}C chemical shift range of peptides and proteins, the ^{13}C carrier will be far off-resonant with respect to the centre of the aliphatic carbon resonances. In this context we have simulated for the

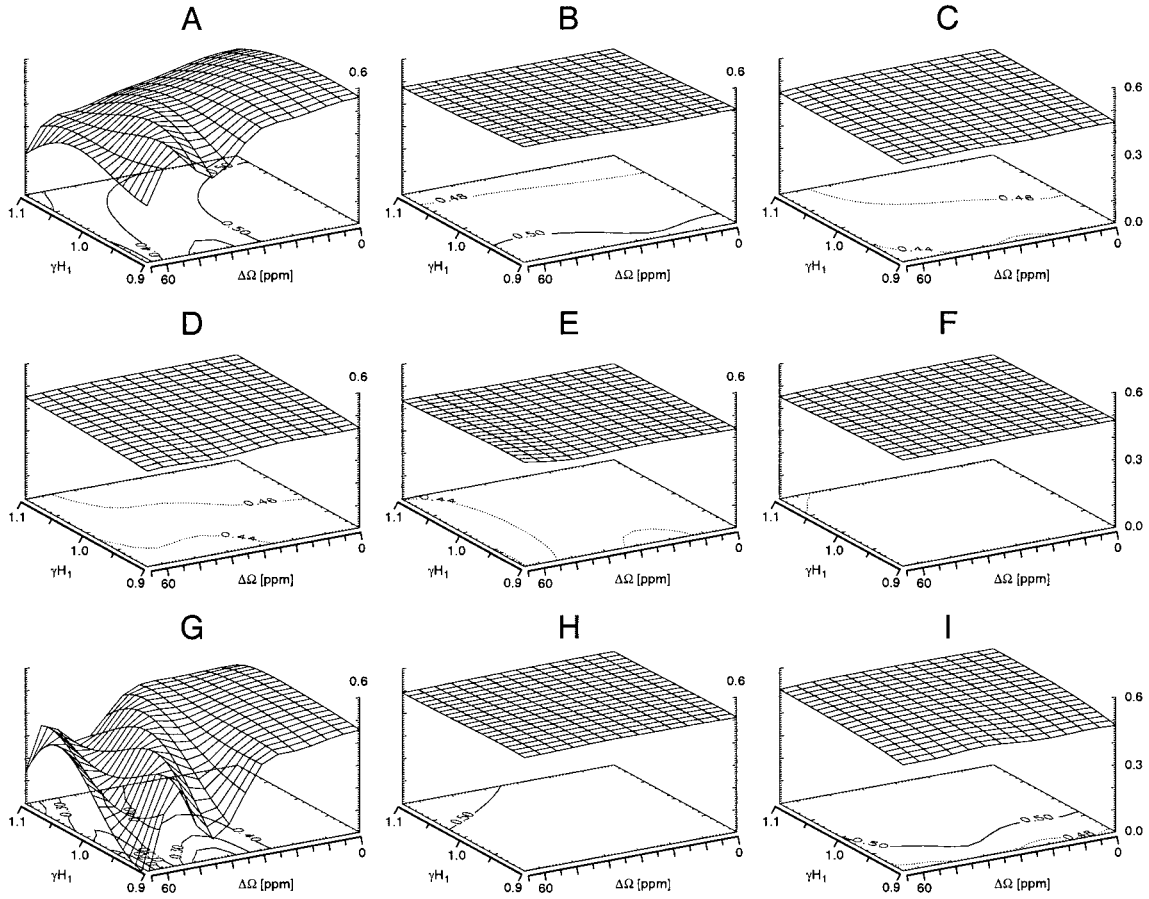

Figure 6. Transferred signal amplitude on the second spin ($^{13}C^{\beta}$) starting with z magnetisation on spin 1 ($^{13}C^{\alpha}$) at zero recoupling time. These plots (800 MHz) show the dependence of the transferred magnetisation as a function of the resonance offset $\Delta\Omega$ (defined in ppm as the difference between the carrier frequency and the centre of the $^{13}C^{\alpha}$ and $^{13}C^{\beta}$ resonances in alanine) and over a range ($\pm$ 10%) of the ^{13}C RF field strength employed. Simulations were carried out at a spinning speed of 15 000 Hz unless indicated otherwise. (A) rectangular pulse (13.4 μs, xy-8, 37.3 kHz γH_1, $t_{mix} = 2.13$ ms), (B) tanh/tan pulse (40 μs, xy-8, 37.3 kHz γH_1, $t_{mix} = 2.13$ ms), (C) tanh/tan pulse (40 μs, p5d, 37.3 kHz γH_1, $t_{mix} = 2.67$ ms), (D) tanh/tan pulse (40 μs, p5dp$\overline{5d}$, 37.3 kHz γH_1, $t_{mix} = 2.67$ ms), (E) tanh/tan pulse (60 μs, p5d, 30.0 kHz γH_1, $t_{mix} = 2.27$ ms, 11 000 Hz), (F) cagauss pulse (80 μs, p5d, 42 kHz γH_1, $t_{mix} = 2.27$ ms, 11 000 Hz), (G) rectangular pulse (13.4 μs, xy-8, 37.3 kHz γH_1, $t_{mix} = 4.27$ ms), (H) tanh/tan pulse (40 μs, xy-8, 37.3 kHz γH_1, $t_{mix} = 4.27$ ms) and (I) tanh/tan pulse (40 μs, p5d, 37.3 kHz γH_1, $t_{mix} = 4.0$ ms). All other parameters are as in Figure 2.

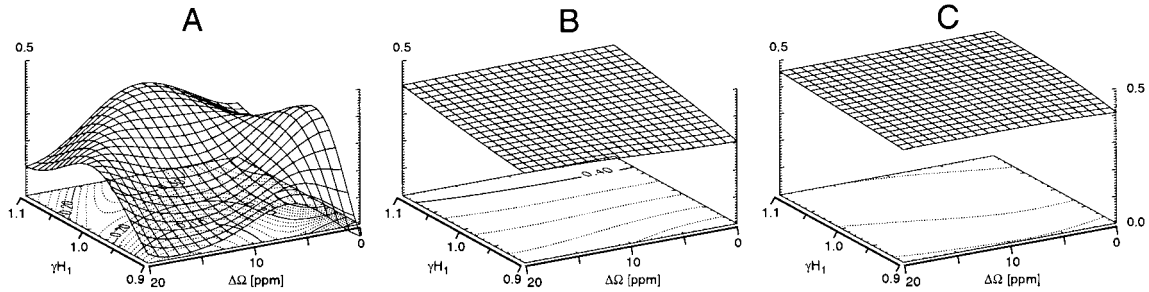

Figure 7. Transferred signal amplitude on the second spin ($^{13}C'$) starting with z magnetisation on spin 1 ($^{13}C^{\alpha}$) at zero recoupling time. These plots (800 MHz) show the dependence of the transferred magnetisation as a function of the resonance offset $\Delta\Omega$ (defined in ppm as the difference between the carrier frequency and the centre of the $^{13}C^{\alpha}$ and $^{13}C'$ resonances in glycine) and over a range ($\pm$10%) of the ^{13}C RF field strength employed. Simulations were carried out at a spinning speed of 15 000 Hz. (A) rectangular pulse (13.4 μs, xy-8, 37.3 kHz γH_1, $t_{mix} = 4.27$ ms), (B) tanh/tan pulse (40 μs, xy-8, 37.3 kHz γH_1, $t_{mix} = 4.27$ ms), (C) tanh/tan pulse (40 μs, p5d, 37.3 kHz γH_1, $t_{mix} = 4.0$ ms).

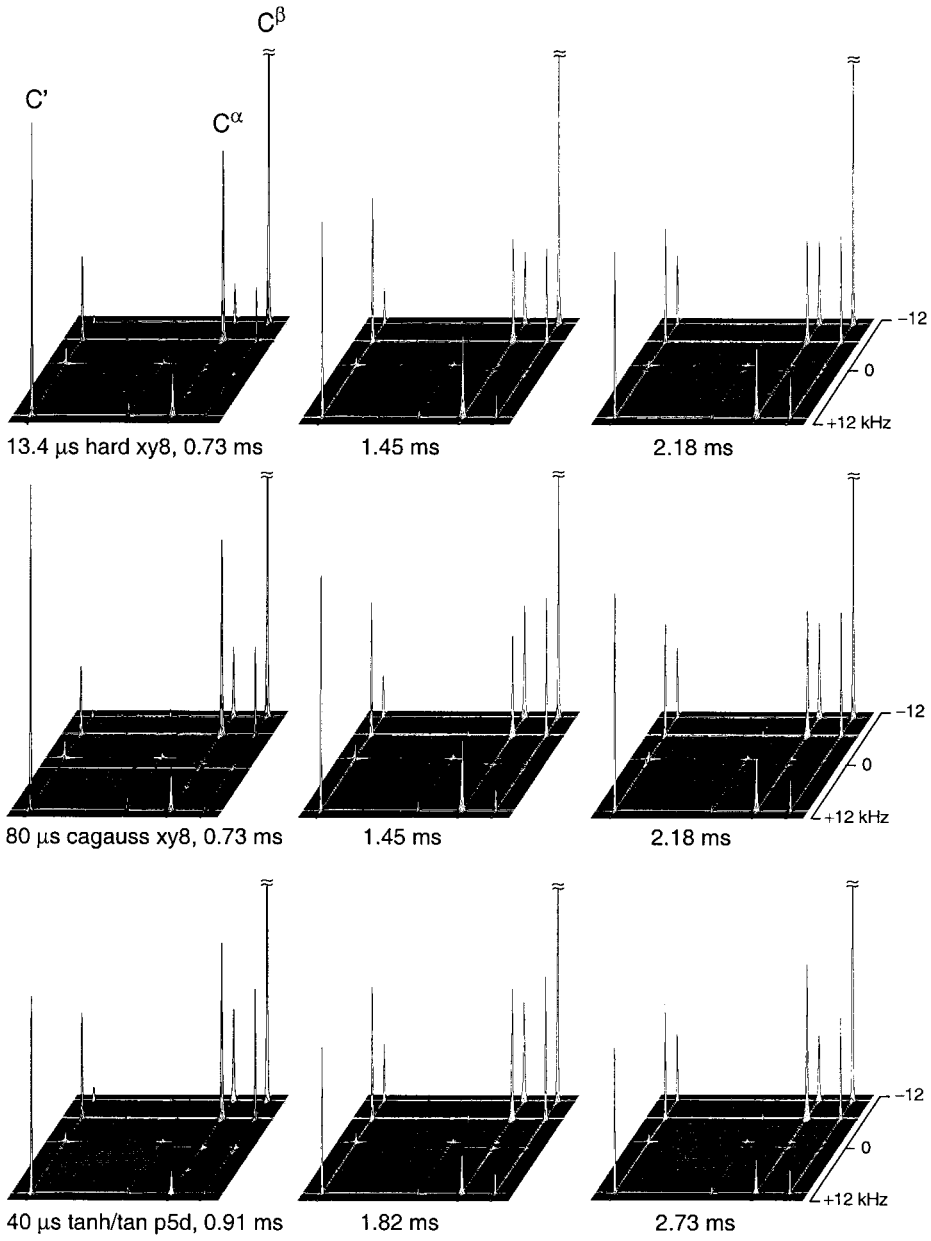

Figure 8. 2D RFDR spectra (zoomed plots) of uniformly labelled alanine at a spinning speed of 11 000 Hz obtained employing ^{13}C recoupling RF pulse parameters and mixing times indicated. The data were generated with 13.4 μs rectangular pulses of 37.3 kHz γH_1, 80 μs cagauss pulses of 42.0 kHz γH_1 and 40 μs tanh/tan of 37.3 kHz γH_1 employing a spectral width of 50 kHz in both dimensions, 256 t_1 increments and a recycle delay of 2 s. All spectra were collected by keeping the RF carrier at the middle of the ^{13}C resonances. For each of the pulses, all spectra are plotted at the same threshold/vertical scale.

case of $C^{\alpha} \rightarrow C^{\beta}$ magnetisation transfer the dependence of the amplitude of the transferred longitudinal magnetisation, as a function of the resonance offset $\Delta\Omega$ (defined as the difference between the carrier frequency and the centre of the $^{13}C^{\alpha}$ and $^{13}C^{\beta}$ resonances in alanine). Figure 6 shows a few representative plots of this dependence. These plots, shown for different mixing times, correspond to a spinning speed of 15 000 Hz and a field strength of 800 MHz. The plots with the rectangular pulses of 13.4 μs duration were generated employing the xy-8 phasing scheme while those for the adiabatic pulses were obtained with the xy-8/p5d/p5dp$\overline{5d}$ schemes as detailed in the figure caption. The plots given in Figure 6 also show the effect of small variations in the ^{13}C RF field strength employed on the RFDR performance. The simulations for the rectangular pulse shown in Figure 5 indicate that by keeping the ^{13}C RF carrier in the middle of the aliphatic region it may be possible to obtain reasonably satisfactory 2D chemical shift correlation data for the aliphatic carbons at high fields (Pauli et al., 2000, 2001). However, the simulations for the rectangular pulse shown in Figure 6 clearly suggest that at high magnetic fields the cross peak intensities will be significantly reduced if 2D chemical shift correlation is recorded in the entire ∼180 ppm range (McDermott et al., 2000). As in Figure 6, Figure 7 shows a few representative plots of the resonance offset dependance of the amplitude of the transferred longitudinal magnetisation in the $C^{\alpha} \rightarrow C'$ case employing rectangular (13.4 μs, xy-8) and tanh/tan (40 μs, xy-8, p5d) pulses. In the presence of resonance offset and H_1 inhomogeneity, Figure 6 and 7 clearly indicate that, in agreement with our earlier experimental studies, the performance of RFDR with adiabatic pulses will be clearly superior.

Besides our recent studies (Heise et al., 2002), we have carried out additional experimental measurements to validate the conclusions arrived here through numerical simulations. Figure 8 shows, as a function of the dipolar recoupling time, some representative 2D ^{13}C chemical shift correlation spectra of alanine recorded at a spinning speed of 11 000 Hz, a field strength of 500 MHz and employing rectangular (13.4 μs, xy-8), cagauss (80 μs, xy-8) and tanh/tan (40 μs, p5d) inversion pulses. These spectra were recorded by keeping the ^{13}C RF carrier at the middle of the spectral range and the data shown are in general agreement with what is expected from the simulations (Figures 2–4). With the rectangular inversion pulses, the $C^{\alpha} \rightarrow C'$ transfer is faster than the $C^{\alpha} \rightarrow C^{\beta}$ transfer and with the adiabatic pulses, as expected, the rate of buildup of the $C^{\alpha} \rightarrow C^{\beta}$ cross peak is slightly faster than the rate of buildup of the $C^{\alpha} \rightarrow C'$ cross peak intensity.

The simulations carried out at 800 MHz (Figure 6) suggest, as mentioned above, that at high fields and with large resonance offsets the $C^{\alpha} \leftrightarrow C^{\beta}$ cross peak intensities in spectra generated employing rectangular inversion pulses will be significantly reduced in comparison to the intensities in spectra obtained with adiabatic inversion pulses. We have experimentally demonstrated this, using the available 500 MHz spectrometer, by carrying out RFDR experiments in the absence and in the presence of a large carrier offset, keeping the RF carrier at the centre of the ^{13}C spectral range or 10 kHz away, respectively. Figure 9 shows 2D RFDR spectra of uniformly labelled alanine generated without and with the carrier offset employing rectangular and adiabatic inversion pulses. As expected, in the presence of large resonance offset the $C^{\alpha} \leftrightarrow C^{\beta}$ direct and $C^{\beta} \rightarrow C^{\alpha} \rightarrow C'$ relayed cross peak intensities in the spectrum recorded with the rectangular 180° pulse have significantly reduced amplitudes compared to that obtained with the adiabatic pulse. The experimental data shown in Figure 9 is in general agreement with the simulations shown in Figure 6 and with our earlier experimental studies (Heise et al., 2002). The improved performance in the presence of large resonance offset clearly points to the potential utility of adiabatic inversion pulses for obtaining ^{13}C chemical shift correlation spectra in the entire range of ^{13}C chemical shifts at high fields. Besides the tanh/tan and cagauss adiabatic pulses, we have also obtained chemical shift correlation spectra of alanine (data not shown) employing other adiabatic pulses such as the 'cacos' inversion pulses (Kupce and Freeman, 1996). The rate of buildup of cross peak intensities with such pulses is similar to that seen with the tanh/tan and cagauss pulses and in the presence of resonance offset, in general, the performance of RFDR with adiabatic pulses is found to be superior to the performance with the rectangular inversion pulse.

Figure 10 shows 2D ^{13}C chemical shift correlation spectra of alanine recorded at a spinning speed of 11 000 Hz, a field strength of 500 MHz, a dipolar mixing time of 2.18 ms and employing tanh/tan adiabatic pulses of 40, 50, 60 and 70 μs duration with the xy-8 phasing scheme. The corresponding data obtained with 13.5 μs rectangular and 80 μs cagauss inversion pulses can be seen in Figure 8. At the mixing time employed, the variations in the $C^{\alpha} \rightarrow C^{\beta}$ and $C^{\alpha} \rightarrow C'$

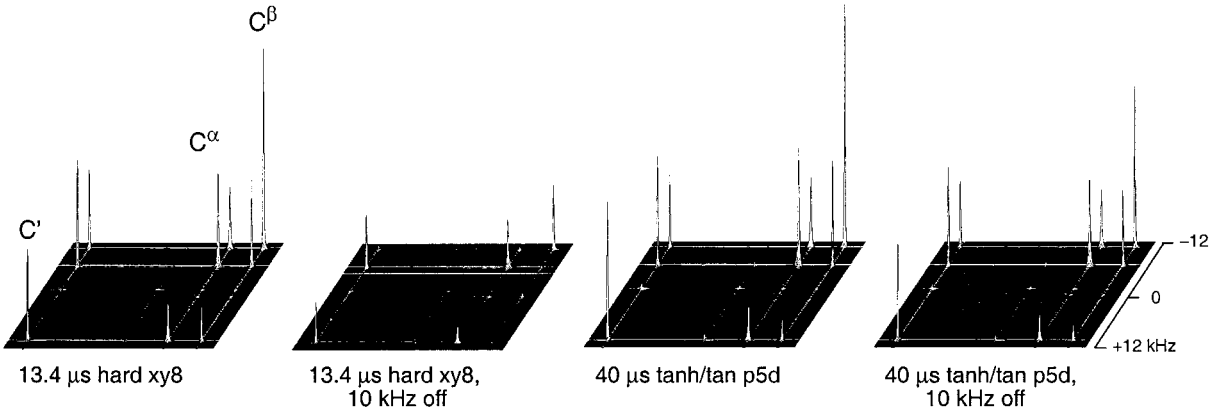

Figure 9. 2D RFDR spectra (zoomed plots) of uniformly labelled alanine at a spinning speed of 11 000 Hz obtained employing ^{13}C recoupling RF pulse parameters and resonance offset indicated. Here, the resonance offset is defined as the difference between the carrier frequency (shifted towards the carbonyl resonance) and the middle of the ^{13}C spectral width. The data were generated with rectangular (13.4 μs, xy-8, 37.3 kHz γH_1, $t_{\mathrm{mix}} = 5.81$ ms) and tanh/tan (40 μs, p5d, 37.3 kHz γH_1, $t_{\mathrm{mix}} = 5.45$ ms) inversion pulses employing a spectral width of 50 kHz in both dimensions, 256 t_1 increments and a recycle delay of 2 s. All spectra are plotted at the same threshold/vertical scale.

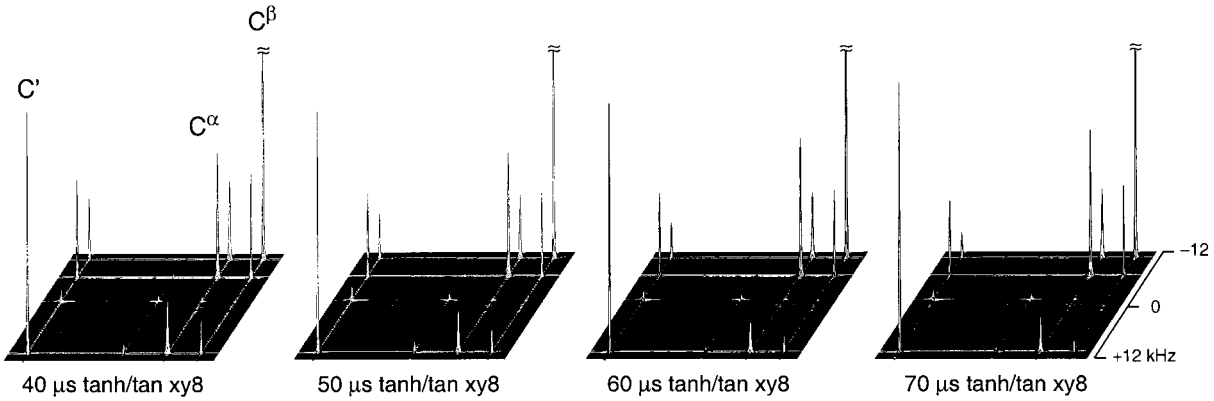

Figure 10. 2D RFDR spectra (zoomed plots) of uniformly labelled alanine at a spinning speed of 11 000 Hz obtained employing ^{13}C tanh/tan adiabatic pulse parameters indicated. Spectra were generated ($t_{\mathrm{mix}} = 2.18$ ms, xy-8) with pulses of durations of 40.0 μs at 37.3 kHz, 50 μs at 33 kHz, 60 μs at 30 kHz and 70 μs at 30 kHz γH_1, employing a spectral width of 50 kHz in both dimensions, 256 t_1 increments and a recycle delay of 2 s. All spectra are plotted at the same threshold/vertical scale as shown for the rectangular and cagauss pulses in Figure 8.

cross peak intensities are approximately in agreement with those expected from the simulations given in Figure 4. For example, the cross peak intensities obtained with 80 μs cagauss pulses are larger than those obtained with 70 μs tanh/tan pulses and with increase in the duration of the tanh/tan pulses the $C^{\alpha} \rightarrow C^{\beta}$ cross peak intensities decrease at the mixing time employed. It is worth mentioning that, in situations where correlation spectra of only the aliphatic region are needed at high fields, it is possible to minimize the cross-talk between decoupling and recoupling RF fields by using long tanh/tan adiabatic inversion pulses as they require less RF power. The reasonably satisfactory agreement between the 500 MHz two-spin simulations and experimental data suggests that the simulations given in our paper are highly relevant for obtaining 2D ^{13}C chemical shift correlation data via RFDR in uniformly labelled peptides/proteins at high fields.

The optimal RF field strength to be employed with adiabatic pulses and the chemical shift range over which 2D correlation data of good quality can be generated is easily obtained experimentally. This is achieved by monitoring, for satisfactory RFDR performance, the observed signal as a function of the adiabatic ^{13}C pulse power level and carrier offset. In our studies, to avoid probe arcing at higher power levels, we have employed a decoupling power level of the order of 90 kHz and we have used only the minimum experimentally required recoupling power levels. In situations where compensation for H_1 in-

homogeneity is required, higher recoupling and decoupling power levels may be needed. With tanh/tan pulses of 30 μs duration we have seen experimentally (data not shown) that efficient RFDR performance over a large bandwidth and with long mixing times requires a ^{13}C RF field strength of $\sim$ 47 kHz and a ^{1}H decoupling field strength of $\sim$ 120 kHz or higher. With the availability of higher decoupling field strengths in the current generation of MAS probes, it should be feasible to execute RFDR with such short adiabatic pulses without any loss of polarization due to cross talk between the decoupling and recoupling channels.

Procedures for obtaining efficient ^{13}C chemical shift correlation data at high fields have been reported at very fast magic angle spinning frequencies (Ishii, 2001; Brinkmann et al., 2002). The results presented in this work clearly illustrate the potential of RFDR with short adiabatic inversion pulses to obtain efficient correlation spectra in the entire range of carbon chemical shifts in uniformly labelled biological systems, at the currently available high magnetic fields and at MAS frequencies $<$ 20 kHz. In situations where it is required to generate correlation data in the aliphatic region only, our studies reveal that it is possible to minimise interference between the decoupling and recoupling fields by the use of adiabatic pulses of long duration without compromising the efficacy of RFDR. Our study also shows that the cross peak intensities seen in the chemical shift correlation spectra obtained with adiabatic inversion pulses are not strongly sensitive to chemical shift differences. Results from numerical simulations also suggest that at high magnetic fields, it is possible to obtain good chemical shift correlation data by employing adiabatic inversion pulses with the phasing scheme p5d {0°, 240°, 240°, 60°, 0°}, even with long dipolar mixing times. Although found to be effective for RFDR experiments, phasing schemes such as this have been originally designed to achieve broadband inversion of longitudinal magnetisation. Currently, work is in progress to find improved phasing schemes for further enhancing the performance of RFDR with adiabatic pulses by directly maximising the efficieny of longitudinal magnetisation transfer via numerical optimisation procedures. The results from these investigations will be reported elsewhere.

References

Bak, M. and Nielsen, N. (1997) *J. Magn. Reson.*, **125**, 132–139.

Bak, M., Rasmussen, J.T. and Nielsen, N.C. (2000) *J. Magn. Reson.*, **147**, 296–330.

Baum, J., Tycko, R. and Pines, A. (1985) *Phys. Rev.*, **A32**, 3435–3447.

Bennett, A.E., Ok, J.H., Griffin, R.G. and Vega, S. (1992) *J. Chem. Phys.*, **96**, 8624–8627.

Bennett, A.E., Rienstra, C.M., Griffiths, J.M., Zhen, W., Lansbury, P.T. and Griffin, R.G. (1998) *J. Chem. Phys.*, **108**, 9463–9479.

Boender, G.J., Raap, J., Prytulla, S., Oschkinat, H. and de Groot, H.J.M. (1995) *Chem. Phys. Lett.*, **237**, 502–508.

Brinkmann, A., Schmedt auf der Günne, J. and Levitt, M.H. (2002) *J. Magn. Reson.*, **156**, 79–96.

Fujiwara, T. and Nagayama, K. (1988) *J. Magn. Reson.*, **77**, 53–63.

Gullion, T., Baker, D.B. and Schaefer, J. (1990) *J. Magn. Reson.*, **89**, 479–484.

Heise, B. (2001) PhD Thesis, Friedrich-Schiller-Universität Jena.

Heise, B., Leppert, J., Ohlenschläger, O., Görlach, M. and Ramachandran, R. (2002) *J. Biomol. NMR*, **24**, 237–243.

Heise, B., Leppert, J. and Ramachandran, R. (2000) *J. Magn. Reson.*, **146**, 181–187.

Hwang, T., van Zijl, P.C.M. and Garwood, M. (1998) *J. Magn. Reson.*, **133**, 200–203.

Ishii, Y. (2001) *J. Chem. Phys.*, **114**, 8473–8483.

Kupce, J. and Freeman, R. (1995) *J. Magn. Reson.*, **A117**, 246–256.

Kupce, J. and Freeman, R. (1996) *J. Magn. Reson.*, **A118**, 299–303.

Lehmann, M.S., Koetzle, T.F. and Hamilton, W.C. (1972) *J. Am. Chem. Soc.*, **94**, 2657–2660.

Leppert, J. (2001) PhD thesis, Friedrich-Schiller-Universität Jena.

Leppert, J., Heise, B., Görlach, M. and Ramachandran, R. (2002) *J. Biomol. NMR*, **23**, 227–238.

McDermott, A., Polenova, T., Bockmann, A., Zilm, K.W., Paulsen, E.K., Martin, R.W. and Montelione, G.T. (2000) *J. Biomol. NMR*, **16**, 209–219.

Pauli, J., Baldus, M., van Rossum, B., de Groot, H. and Oschkinat, H. (2001) *ChemBioChem*, **2**, 272–281.

Pauli, J., von Rossum, B., Förster, H., de Groot, H.J.M and Oschkinat, H. (2000) *J. Magn. Reson.*, **143**, 411–416.

Tannus, A. and Garwood, M. (1996) *J. Magn. Reson.*, **A120**, 133–137.

Tycko, R., Pines, A. and Guckenheimer, J. (1985) *J. Chem. Phys.*, **83**, 2775–2802.

van Rossum, B., Schulten, E.A.M., Raap, J., Oschkinat, H. and de Groot, H.J.M (2002), *J. Magn. Reson.*, **155**, 1–14.

Zaborowski, E., Zimmermann, H. and Vega, S. (1999) *J. Magn. Reson.*, **136**, 47–53.